# Detailed Investigation of Light Induced Charge Injection into a Single Conjugated Polymer Chain

**Josh Bolinger, Kwang-Jik Lee, Rodrigo E. Palacios, and Paul F. Barbara***

*Center for Nano and Molecular Science and Technology, University of Texas, Austin, Texas 78712*

*Received: June 03, 2008; Revised Manuscript Received: July 30, 2008*

Detailed single molecule spectroscopic results are presented for the recently reported oxidation of single-chain conjugated polymers of MEH-PPV at the HTL/insulator interface of an MIS device. The charge injection process was determined to be light dominated with no charging occurring in the dark at any applied bias. The nature of the optical preparation of the injected charge is explored by a range of single molecule fluorescence voltage modulation techniques. The observed charging dynamics are highly consistent with a cooperative charging effect. It is also observed that analogous charging occurs for the conjugated polymer F8BT.



## 1. Introduction

Positive charge carriers (holes) have been broadly reported to be energetically trapped in organic materials and devices. However, the consequences of charge trapping and the nature of the trapping process itself remains poorly defined, despite decades of investigation. For example, the poly(phenylene vinylene) (PPV) class of polymers form shallow and deep traps with energies of 0.1−0.2 and 0.6−0.8 eV, respectively, above the highest occupied molecular orbital levels of these polymers.[1−3] The consequences of positive charge trapping in the layers of organic devices are difficult to predict; indeed large enhancement[4,5] and degradation[6,7] of device performance have been reported in different cases. Previous work on devices comprised of conjugated polymers in organic light emitting diodes (OLEDs) and thin film transistors (TFTs) have shown that deep hole trapping is a common phenomena in organic electronics.

Reports of charge trapping in F8BT OLEDs have been observed where the continuous driving of a device resulted in the steadily increasing efficiency of the LED over time.[4] The enhancement was found to persist for up to 24 h if the device was stored in a nonbiased state. The enhancement was attributed to charge trapping at the hole injection electrode interface where holes become deeply trapped. It was further proposed that deeply trapped holes (DTH) paired with electrons are responsible for interfacial dipoles that distort the hole transport band sufficiently to allow for tunneling injection of holes and also enhancement of electron injection at the nearby electron injection electrode. In a different example, polythiophene thin-film-transistors (TFTs) have been reported to exhibit current loss due to hole trapping, which reduces the number of mobile carriers in the transistor channel.[6,8] Using the current-loss as an indirect measurement of hole trapping, it was determined that the stressing rate as defined by the threshold voltage shift was proportional to the initial hole concentration. Electron force microscopy (EFM) measurements performed on pentacene TFT's have shown that trapped holes are highly localized within the device and the rates of formation of these trapped charges are delayed relative to the application of the gate bias and are strongly dependent on the initial concentration of shallow holes.[9,10]

Several mechanisms for the formation of hole traps have been proposed. Chemical doping of the organic layer has been suggested as a source for DTH. Possible contaminants such as $O_2$ and $H_2O$, residual impurities from the synthesis, and ion migration from other layers have been implicated in the formation of trap sites.[1−3,11−18] Others suggest that the trapping occurs due to interfacial surface sites located within the device.[5,19,20] A distinct alternative is that the traps are an intrinsic property of the material. Some of the proposed mechanisms for the origin of intrinsic traps include molecular rearrangement, bipolaron formation, and midgap-state filling.[6,8−10,21−25]

We have recently reported that trapped holes can be formed by a light-injected hole transfer mechanism (LIHT) in a single conjugated polymer chain as monitored by fluorescence-voltage single molecule spectroscopy (F-V/SMS) techniques.[26] The light assisted charge injection was shown to be highly cooperative with regard to the number of injected holes, implying the need for the reorganization of the polymer system to accommodate the charge, indeed it was observed that all charge injection into single chain polymers occurs through light aided injection. The LIHT may be responsible for the poorly understood build up of trapped charge in some organic electronic devices, and this effect may have important consequences for the rate of charge injection and overall device efficiency in OLED device performance. It is interesting to note that the intensities used in our experiments result in excitation rates similar to those witnessed in state of the art OLEDs.[26] Our report may be related to the report of the light driven nature of trap filling in certain conjugated polymers,[5] i.e., OLEDs comprised of MEH-PPV films were shown to undergo device enhancement following a brief treatment with white light illumination while being forward biased. This enhancement has been attributed to deep trap filling near the anode and the resulting space charge aided in electron injection into the device by lowering the Schottky barrier present at that interface, helping to balance the mobile carriers in the device, improving recombination in the emitting layer.

In this paper, we present new fluorescence-voltage single molecule spectroscopy (F-V/SMS) results on hole injection into conjugated polymers. We also analyze and discuss the previously reported data from our group in much greater detail.

* To whom correspondence should be addressed. E-mail p.barbara@mail.utexas.edu.

10.1021/jp804901s CCC: $40.75 
Published on Web 11/04/2008

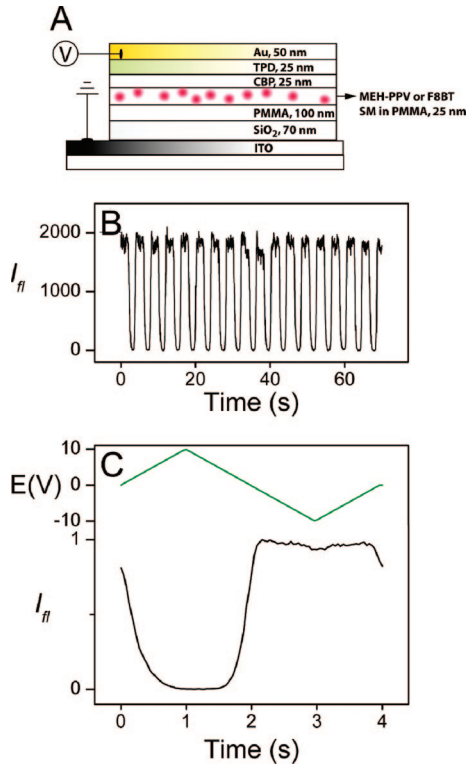


**Figure 1.** (A) Schematic of the hole-injection device structure used in these experiments. (B) Single molecule fluorescence intensity transient obtained while modulating the bias across the device. (C) Time averaged fluorescence intensity transient derived from the data shown in (B). The green line represents one cycle of the applied bias (scan rate of 10 V/s) in the experiment. The presented curve is an average of 40 4-s cycles using a light intensity of 6 W/cm$^2$.

## 2. Experimental Section

**2.1. Sample Preparation.** The hole injection devices utilized a large area (1 cm$^2$) multilayer metal−insulator−semiconductor (MIS) structure as shown in Figure 1A. The device was fabricated bottom-up on top of a patterned indium tin oxide (ITO) coated coverslip (Evaporated Coatings Inc., sheet resistance of 110 Ω). The dielectric layer was $SiO_2$, grown with inductively coupled plasma chemical vapor deposition (ICP-CVD) (Oxford instruments, Plasmalab 80plus) at 200 °C with a thickness of 70 nm through a shadow mask. Poly(methyl methacrylate) (PMMA, Sigma Aldrich, $M_w = 101$ kg/mol) and poly(2-methoxy-5-(2′-ethylhexyloxy)1,4-phenylenevinylene) (MEH-PPV, Uniax, $M_w = 1000$ kg/mol) were deposited by spin casting from toluene. The bottom PMMA layer served to isolate MEH-PPV from the $SiO_2$ layer. Previous work done on a similar system with $SiO_2$ that was deposited via ebeam evaporation reports an inherent photoinstability of single molecules at the $SiO_2$ surface. Single chain MEH-PPV was imbedded in a 25-nm thick host matrix of PMMA to prevent aggregation, and the concentration of MEH-PPV was adjusted such that the areal density of the fluorophore was 0.5 molecules/$\mu$m$^2$. The hole transport layers 4,4′-*N*,*N*′-dicarbazole-biphenyl (CBP) (Sigma Aldrich) and *N*,*N*′-bis(3-methylphenyl)-*N*,*N*′-diphenylbenzidene (TPD) (Sigma Aldrich) were employed in these devices. Both hole transport layers were deposited with thermal deposition under high vacuum ($10^{-6}$ Torr) at a rate of 1 Å/s for a thickness of 25 nm for each. Comparison devices were fabricated with 50-nm layers of TPD as the only HTL. Gold was chosen for the top contact and was also thermally deposited with a typical rate of 2 Å/s. Patterning of all the thermally deposited layers was accomplished through the use of shadow masks. The resulting devices contained four independent 15-mm$^2$ active areas.

All device fabrication was performed in a glovebox environment ($O_2$ and $H_2O$ concentrations below 5 ppm) except for the $SiO_2$ deposition where exposure of the substrate to atmosphere was necessary. Devices were wired inside the glovebox using silver paint and then packaged using epoxy and a coverslip. When unsealed devices were interrogated, the single molecule fluorescence showed a gradual photobleaching whose rate was found to be strongly light dependent. Packaging of the devices lead to enhanced single molecule fluorescence stability, allowing for individual molecules to be studied for more than an hour without significant photobleaching being observed. All devices were immediately returned to the glovebox following interrogation as it was found that devices left out in ambient atmosphere overnight showed single molecule fluorescence decay similar to unsealed samples. This effect has been observed before and is attributed to slow $O_2$ and $H_2O$ diffusion through the epoxy seal.[27]

**2.2. Confocal Apparatus.** Single molecule microscopy has been previously reported[28] and is only briefly described here. Studies were performed using an inverted confocal microscope (Zeiss, Axiovert 100), and optical excitation was provided with the 488-nm line of a Ar Kr ion laser (Melles Griot, model 35 LTL 835) that was filtered (488 interference filter, Chroma) and attenuated with neutral density filters. Circularly polarized light was used to excite all axes of the molecules in the XY plane and was provided by passing the laser through a quarter-wave plate (CVI Laser). The light was focused to a diffraction limited spot size of 270 nm with a 100× oil immersion objective (Zeiss, Achrostigmat 1.25 NA). Excitation scatter from the sample was filtered using an appropriate dichroic mirror and filter (Chroma, 488 nm notch filter). Fluorescence detection was performed using avalanche photodiodes (APDs) (Perkin-Elmer, SPCM-AQR-15). Image acquisition was performed through the use of a closed loop piezoelectric $x-y$ stage (Queensgate, NPS-100A) driven by a computerized controller (RHK, SPM1000). The acquired images were then used to locate single molecules so that the stage could then be moved to excite individual molecules in the device.

Bias modulation of the single molecule device was accomplished with the use of a programmable function generator (Wavetek, model 29A). Light intensity modulation experiments were accomplished through the use of acousto-optical modulators where the input electronic signal to the modulator was provided by another programmable function generator. A master function generator was used to synchronize both the bias generator, the light waveform, and a multichannel scalar board (MCS) that was used to read the output from the APD. Two separate MCS boards were used in this experiment; a Becker Hickl PMS-400 was used to take long-time nonaveraged measurements to verify that the fluorescence of the single molecule being irradiated was stable, and a FAST ComTec Gmbh MCA-3 was used to take time-averaged measurements to achieve high signal-to-noise.

## 3. Results and Discussions

**3.1. FV/SMS Measurements of Hole Injection.** This laboratory introduced FV/SMS techniques as a method to indirectly monitor charge injection via fluorescence quenching in specially designed devices suitable for single molecule spectroscopy.[29] The devices used in FV/SMS are adapted from conventional metal−insulator−semiconductor (MIS) capacitors with single

molecule conjugated polymers located at the interface of the semiconductor and the insulator. The semiconductors used are common organic hole transport materials where, upon application of a positive bias, holes are injected from the anode and flow through the HTL to the insulator interface. With a sufficiently high concentration of holes at the insulator interface, controllable injection into the single chain polymer molecules can occur. CBP was chosen for its relatively high ionization potential (IP) of 5.9−6.3 eV[30−33] while TPD has an IP of 5.6 eV[34,35] and was used to act as an intermediate step between the Au electrode and the CBP HTL. Reversal of the applied bias results in the removal of the accumulated charge, reducing the polymer to its original state. The Au injecting electrode prevents electron injection into the device at the negative biases used in this experiment due to the high work function of gold and the low electron affinity of the HTLs. Since holes are a well documented source of fluorescence quenching in conjugated polymers, the use of single molecule fluorescence quenching can be used to indirectly monitor charge injection.[29,36−40]

Figure 1B and C demonstrates the effect of a periodic triangular bias applied across one of these CBP MIS devices on the fluorescence of a single molecule. The bias-induced quenching is highly reproducible occurring repeatedly for thousands of cycles for a single chain. Consistent with previous results,[29,40,41] positive bias coincides with fluorescence quenching, while negative bias coincides with fluorescence recovery. The quenching has been assigned to the injection of positive charge from the HTL. It has been shown that one hole induces quenching of ∼40% of the original fluorescence intensity for MEH-PPV single molecules of this molecular weight suggesting that the near complete quenching of the single molecule fluorescence is due to the injection of 7−8 charges.[38,40] The bias dependence of the hole injection rate and yield is attributed to the bias dependence of the concentration of holes at the CBP HTL interface, which decreases tremendously at negative bias in this CBP MIS device. The percentage of molecules in each device that demonstrated bias modulated fluorescence was ∼95% and the observed modulation was highly reproducible from device to device and from molecule to molecule demonstrating good electrical contact between the single conjugated polymer chain and the CBP HTL. The observations reported herein are qualitatively different than previous reports on devices without a good hole injection layer. i.e. CBP. Without this layer the observed fluorescence modulation is apparently due to a pure electric field effect rather than hole injection or in some cases, hole injection due to oxygen and/or multiphoton ionization.[42−46]

As further evidence that quenching is the result of charge injection, insulating layers of either $SiO_2$ deposited by ebeam evaporation or poly(isobutyl methacrylate) spun cast from an orthogonal solvent were placed between the MEH-PPV and the CBP HTL. The incorporation of these layers completely arrests fluorescence modulation in the majority of the molecules (<5% of molecules modulate, data not shown), and the few molecules that do show fluorescence modulation in these control devices show erratic modulation behavior suggesting spurious charging and perhaps a pure electric field effect. This supports our conclusion that fluorescence modulation requires electrical contact with the HTL, supporting the idea that modulation is the result of hole injection, not the electric field.

***Sweep-Rate/Light Dependence.*** Figure 2A−C illustrates the dependence of the fluorescence quenching kinetics in the device on the bias scan rate and excitation light intensity. The three F-V curves presented are for the same single molecule under

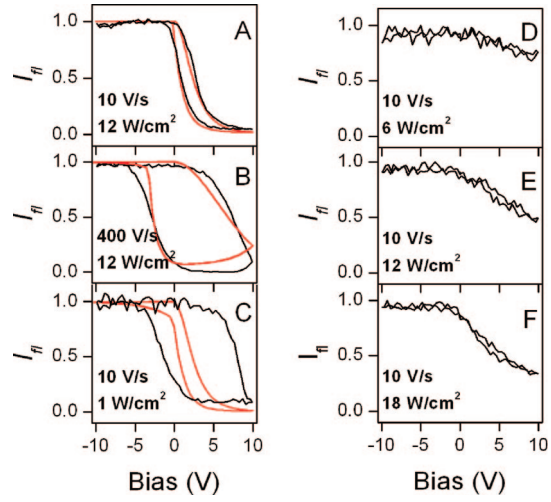


**Figure 2.** (A−C) Time-averaged single-molecule fluorescence-intensity transients (black curves) of MEH-PPV from a CBP device obtained while applying a triangular bias across the device with the bias scan rate and light intensity indicated in the panels for each transient. The red curves represent best fits by the kinetic model detailed in the text. (D−E) Time-averaged single-molecule fluorescence-intensity transients of MEH-PPV from a TPD-only hole injection device obtained while applying a triangular bias. The scan rate and light intensity used for the transients are shown in each panel. Each presented curve is an average of 30−40 cycles. Best fit parameters for (A) $k_F = 1$, $K = 0.01$, $\phi_{PC} = 0.6$; (B) $k_F = 1$, $K = 0.005$, $\phi_{PC} = 0.6$; and (C) $k_F = 0.11$, $k_{EXC} = K = 0.015$, $\phi_{PC} = 0.6$.

different experimental conditions. Analogous behavior is observed for the vast majority of molecules in the sample and, consequently, the ensemble averaged data (not shown) also are similar to the curves in Figure 2A−C. At the slower scan rate of 10 V/s and higher excitation intensity the F-V curves exhibits only a small amount of hysteresis during the bias cycle (Figure 2A). The charge injection process is, therefore, close to being kinetically reversible under these conditions. When the excitation intensity is decreased, however, the F-V curve (Figure 2C) shows clear evidence of hysteresis consistent with the previous proposal that the charge injection process is light driven.[26] At the faster scan rates and higher excitation intensity hysteresis is also clearly observed (Figure 2B). This pure dependence on scan rate may be due to two factors. First, the scan rate may be so rapid that the injection of charges due to light may not be fast enough to keep up with the time varying bias. However, another factor may be slow thermionic charging of the CBP layer. The Schottky barriers for hole transfer across the TPD/CPB heterojunctions may be as large as 0.7 eV according to the HOMO energy offsets.[26] More research will be necessary to distinguish between these two possible explanations for the large hysteresis at the faster scan rates.

***CBP vs TPD.*** F-V/SMS measurements (Figure 2D–F) were performed on TPD only devices with a similar geometry to those of Gesquiere.[29] A comparison of the results to the CBP/TPD devices reveals two important differences. First, for TPD only devices, the quenching depth maxima during a FV scan is light intensity dependent over a large range of biases and scan rates. In contrast, for CBP devices, the quenching depth maxima is always close to 100% for all but the lowest excitation intensities. This implies a lower steady-state concentration of injected holes for TPD vs CBP. This is consistent with energetic considerations (i.e., HOMO energies) for hole transfer across the HTL/MEH-PPV interface which predict that the energetics for hole transfer from TPD into MEH-PPV is isoergic, but exoergic by 0.7 eV for CBP into MEH-PPV. Second, for TPD devices, little or no

hysteresis is observed in the fluorescence quenching and recovery for all excitation intensities and scan rates used in this study. The apparent lack of hysteresis in the TPD only device implies more rapid hole injection and ejection rates than that for CBP. This may be due to shallower hole trapping at the TPD/MEH-PPV interface (as compared to CBP/MEH-PPV) associated with the energetics of hole transfer across the HTL/MEH-PPV interface.

***Kinetic Modeling.*** A light-dependent charging model was developed to simulate the dynamics of the device charging observed for different experimental parameters, i.e. bias scan rate, light intensity, contact resistance, etc. The charge transfer from the Au electrode to the CBP layer is modeled as a diode, resistor and capacitor in series, in analogy to previous circuit treatments involving organic semiconductors.[47−50] The diode is used to model the rectifying properties of the Au/TPD and TPD/CBP interfaces by allowing only hole injection to occur at positive bias and preventing electron injection at negative bias. When the device is sufficiently forward biased, holes can transfer from the Au electrode to the effective capacitor formed between the CBP layer and ITO electrode with a capacitance of ∼1.6 nF, i.e., calculated for a simple parallel plate capacitor model using the geometry of the device.

A differential equation representing the equivalent circuit described above was solved numerically for the application of a triangular wave bias. The result was a $Q_c$ vs time curve where $Q_c$ represents the charge present on the CBP layer and is used as an input for the empirical rate equation that governs the injection and withdrawal of charge from CBP to single molecule MEH-PPV, detailed below. Hole injection from CBP to single-molecule MEH-PPV and the reverse process are treated as chemical reactions that are first order in light intensity and charge concentration at the CBP interface. The rate equation is as follows.

$$\frac{dX_{SM}}{dt} = \frac{k_F k_{EXC} X_C}{1 + \frac{X_{SM}}{\phi_{PC}}} - \frac{K k_F k_{EXC} X_{SM}}{1 + \frac{X_{SM}}{\phi_{PC}}} \quad (1)$$

Here $X_{SM}$ is the mean concentration of charges present on a single molecule of MEH-PPV, $k_F$ is the rate constant for charge photoinjection, $k_{EXC}$ is the rate of photoexcitation of the single molecule (which is proportional to the light intensity), $X_C$ is the charge concentration of the CBP layer, $\phi_{PC}$ is the amount of fluorescence quenching due to one hole on a single MEH-PPV molecule, $K$ is the ratio of the discharge/charge rate constants. This equation was solved using numerical methods, and using the calculated $X_{SM}$, a Stern−Volmer expression was used to convert charge density on the single molecule into fluorescence quenching and plotted against applied bias.

The results of the kinetic simulation are overlaid with the transients presented in Figure 2A−C. For these simulations the effective RC time constant for charging the CBP layer was arbitrarily adjusted to <0.1 s ensuring that at the slower scan rates used in our experiments (10 V/s) the kinetics of charging of the CBP is rapid without a large hysteresis. This further ensures that the hysteresis predicted at slow scan rates by this model is due entirely to rate-limiting photoinduced hole-injection. Since neither TPD nor CBP absorb significantly at the wavelength used for optical excitation, light is expected to only accelerate the charging of MEH-PPV through excited-state electron transfer and not to increase the charging rate of CBP from the Au/TPD layers.

Qualitatively, some of the features in the experimental data are reproduced in the simulations however; the threshold biases

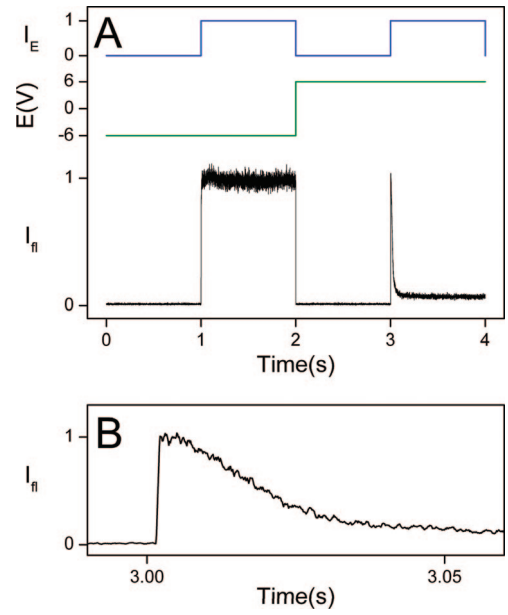


**Figure 3.** (A) Time-averaged single-molecule fluorescence-intensity transient of MEH-PPV (black curve) while simultaneously modulating the applied bias (green curve) and the light (blue curve) as shown. The presented curve is an accumulation of 250 4-s cycles obtained with a light intensity of 0.5 W/cm$^2$. (B) An expanded axis view of the fluorescence transient shown in (A).

at which quenching and recovery are observed to occur vary greatly with scan-rate speed and the light intensity. This aspect of the experimental F-V curves is not well represented by the model as the dominant effects of changing the input is to affect the charging and discharging rate while the threshold bias remains relatively unchanged with respect to the variable parameters of the simulation. These deficiencies in the model suggest that charge injection is much more complicated, supporting the hypothesis of a cooperative mechanism which enhances charge injection.

**3.2. Bias and Excitation Intensity Double Modulation Experiments.** To discern the extent of light induced charging for the single molecule devices, fluorescence intensity experiments were performed using square pulses of light at different biases. The plots shown in Figure 3 portray the sequence and timing of the light and bias pulses and the resulting fluorescence transient. Light pulses that coincide with negative bias give rise to a fluorescence intensity (after a suitable waiting period) that is assigned to MEH-PPV chains without charges, i.e., completely recovered (unquenched). Light pulses that coincide with positive bias give rise to quenching. The intensity of fluorescence signals at negative bias after a suitable time for discharging and at positive bias just after the pulse is applied are the same within experimental errors, suggesting that no charging in the dark has occurred for the single molecules despite the period of positive bias. The results shown here were taken at a bias of 6 V but similar experiments with 10 V also showed no evidence of charge injection without light (data not shown). As a comparison, devices with a 25-nm thick film of bulk MEH-PPV were fabricated and similarly investigated with a multibias pulsed fluorescence experiment suitable for monitoring the quenching dynamics from a film of MEH-PPV.[51] The sequence of bias and light pulses used in this experiment as well as the resulting fluorescence transient is presented in Figure 4. Figure 4A is obtained with constant light illumination while applying the bias shown in the top panel (green curve). It is seen that under constant illumination, as soon as the bias switches from negative

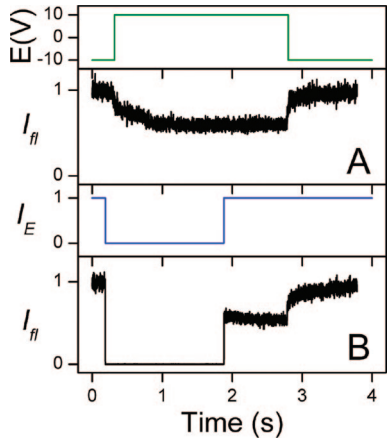


**Figure 4.** Time-averaged fluorescence-intensity transients obtained from an MEH-PPV film device with an applied bias as shown in the upper panel (green curve). The transient shown in panel (A) was acquired with constant light intensity over the course of the entire measurement. The transient in (B) was obtained with a similar applied bias as that of (A) while the light intensity was modulated as shown with the blue curve. Each transient is an average of 4 4-s cycles obtained with a light intensity of 0.1 W/cm$^2$.

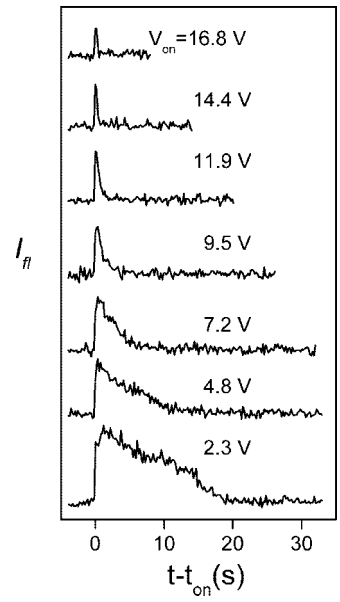


**Figure 5.** Time-averaged fluorescence-intensity transients from a single molecule device. A triangular bias was applied to the device with a scan rate of 20 V/s and the laser excitation intensity (0.2 W/cm$^2$) being introduced to the sample at different biases. Transients are plotted such that $t = 0$ corresponds to when the light pulse was initiated. Each curve is an accumulation of 3−5 cycles

to positive, the fluorescence quenches to a level that is 60% of the original fluorescence intensity within 1 s. Figure 4B is obtained while using the same bias as shown in 4A, however the light sequence used is as shown (blue curve). The data clearly show that while the sample was in the dark and held at positive bias, MEH-PPV underwent thermionic charge injection, resulting in the fluorescence quenching that is immediately observed upon reillumination of the sample. This suggests that the LIHT mechanism is not required for charging of bulk films.

The difference in quenching mechanisms between the single molecule device and the bulk film may be described by the potential difference in the HOMO energies of the two. The HOMO energy level of the bulk CBP and MEH-PPV is reported to be ∼6.0[30−33] and 5.5 eV,[52] respectively. This suggests that injection from CBP to MEH-PPV should be a barrierless process, however in the case of single molecule MEH-PPV, this is not the case. Studies of the ionization potentials of pentacene single molecules vs bulk pentacene show an increase in the HOMO energy level of ∼1.0 eV for the single molecule as compared to the bulk.[53,54] The lowering of the ionization potential of bulk pentacene has been attributed to the large charge screening effect of the surrounding molecules.[54−56] If a similar phenomenon occurs for single-chain MEH-PPV, the resulting Schottky barrier may increase to the point where thermionic injection in the single molecule case is slowed to the point of having a negligible effect on the charge injection, leaving only the LIHT as a means for injection.

To explore the effect of applied bias on the LIHT process, a series of experiments were performed where a triangular bias with a sweep rate of 20 V/s was applied and a single molecule was irradiated at different potentials along the triangular bias with the same light intensity, effectively probing the influence of the charge density on the CBP layer on the quenching dynamics of single molecules. Transients obtained in this experiment are plotted against the time when the light pulse was initiated ($t - t_0$) and are presented in Figure 5. At higher applied bias, it is seen that the rate of quenching increases suggesting that as the CBP layer becomes more charged, the rate of LIHT increases with it. Light intensity was also found to play a similar role in the fluorescence quenching dynamics. As more intense light pulses were used, the fluorescence quenching occurred on a faster time scale; however, regardless of the light intensity used, the quenching depth remained fixed for a given bias. Both of these findings are consistent with the F−V/SMS measurements detailed above and that the LIHT mechanism is comprised of an excited-state charge transfer from the exciton of MEH-PPV and holes in the CBP layer.

***Light-Assisted Detrapping.*** The previous section details how light is necessary for the charging process; however, F−V/SMS measurements suggest that light has a less important role in the discharging process however previous work done on organic electronics suggest light may be a powerful tool in trap decharging.[5,6,23,57] A multibias pulsed experiment was used to elaborate the role of light in the recovery of charged single molecules. Figure 6 presents evidence that light, while not required for the recovery process, significantly enhances it at negative bias. The bias sequence used for this study is detailed in the top panel of Figure 6 (green curve). Both transients (black curves) are shown with their respective light pulse sequences (blue curves) in the panels above them. Briefly, the bias sequence was chosen such that the second period of the negative bias was too short to completely discharge the MEH-PPV molecule as shown by returning the bias back to positive and recharging the molecule. It is seen that when given a short amount of time to discharge, the fluorescence intensity does not fully recover. However, when a brief pulse of light is added to the negative bias, the recovery is shown to be fully complete. Studies performed on charge trapping and bias stress in organic transistors have shown that exposing the system to light of energy above the band gap of the material can greatly enhance the recovery back to the uncharged state of the device.

***Cooperativity and Charge Incubation.*** Figure 3B gives an expanded view of the quenching dynamics observed in the transient from Figure 3A. From this, it is seen that the quenching does not occur immediately following sample illumination. Under the conditions used, there exists a 6-ms delay before quenching begins to occur in the molecule which we refer to as charging incubation. To verify that this delay is real and not due to the kinetics of charging the CBP layer, the delay between

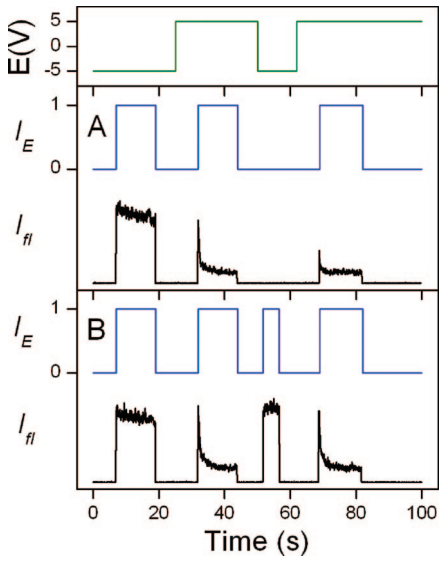


**Figure 6.** Double modulation single-molecule fluorescence-intensity transients (black curves) of a single MEH-PPV molecule. The applied bias for both transients is shown in the top panel (green curve) and the light sequence used is shown directly above each transient (blue curves). Each transient is the accumulation of 10 4-s cycles obtained with a light intensity of 0.5 W/cm$^2$.

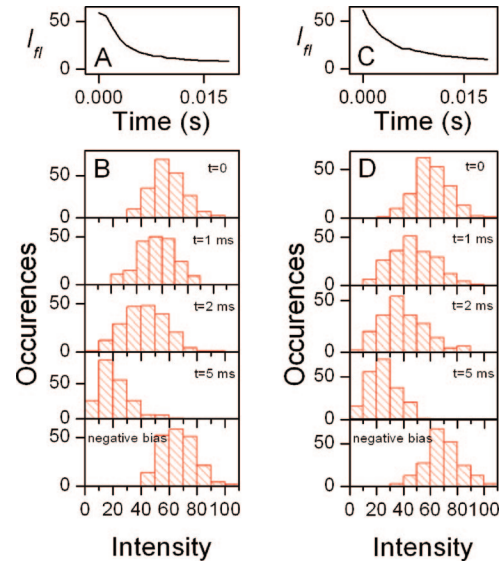


**Figure 7.** (A) Accumulation of 200 single-shot double-modulation single-molecule transients from the same MEH-PPV molecule. The bias and light sequence used are similar to those described in Figure 3. (B) Histograms of experimental single-shot fluorescence intensities at different times after quenching was initiated by a light pulse. (C) 200 accumulated simulation results where the discreet charging of a single molecule is determined via Monte Carlo simulations as described in the text. (D) Histograms of single-shot fluorescence-intensity transients modeled from the Monte Carlo simulations at different times after quenching was initiated. Parameters used for the simulation were $K_F = 1000$, $K_B = 10$, $\phi_{PC} = 0.7$.

the beginning of the positive bias and the light pulse was doubled. This showed no discernible effect on the charging incubation period, ruling out the effects of kinetic charging of the CBP layer. From this, two possible explanations of how charge injection occurs become viable. The first is that the presence of light and charge cause a reorganization of the MEH-PPV single molecule resulting in a lower HOMO energy level similar to that of bulk MEH-PPV. The second is that while light can introduce charge from CBP to MEH-PPV, the charge quickly returns to the CBP layer, and it is only when multiple charges are located in the MEH-PPV that charge becomes trapped, most likely due to bipolaron formation.

***Fluorescence Intensity Fluctuations.*** Using the multibias pulsed technique of Figure 3, hundreds of individual F-t transients were obtained for a single molecule but left unaveraged to obtain the fluctuation in fluorescence intensity at each time point following the onset of quenching. The fluorescence intensity was binned in histograms at different times after the quenching event was observed to begin. The resulting broadening is then a convolution of the shot noise inherent in the measurement and the fluctuation of fluorescence due to the presence of charge. Figure 7A corresponds to the summation of all the experimental transients obtained while Figure 7B corresponds to histograms of the experimentally obtained fluorescence intensities at different times of each individual transient following the onset of quenching. At $t = 0$, defined as when the light pulse is first turned on, the distribution of intensities is centered around 60 counts. At $t = 1$ ms, the distribution is now centered at 50 counts and significant broadening of both the shoulders has occurred. At $t = 2$ ms, the broadening persists and the peak is centered around 40 counts. At $t = 5$ ms, the majority of the quenching has occurred with the peak centered at 20 counts with some residual broadening of the right side of the peak, corresponding to higher counts.

A kinetic model was developed to test the hypothesis that the observed fluorescence quenching in our multibias pulse experiments are the result of a small, discreet number of charges being injected into a single molecule. The model is intended to demonstrate the effect on fluorescence intensity fluctuations by generating a series of transients via a simulation that utilizes a Monte Carlo calculation to determine the number of charges present on a single molecule when conditions are favorable for hole injection, i.e., the CBP layer is charged, light intensity, etc. The probability for increasing ($P_U$) or decreasing ($P_D$) the number of charges located on a single molecule is as follows.

$$P_U = K_F \times \phi_{PC}{}^{C} \times dt \quad (2)$$

$$P_D = K_B \times C \times dt \quad (3)$$

Where $K_F$ is the rate constant for charge injection from CBP to single-molecule MEH-PPV, $\phi_{PC}$ is the amount of fluorescence quenching due to one hole on a single MEH-PPV molecule, C is the charge present on the single molecule, dt is time interval used in the Monte Carlo calculation, and $K_B$ is the discharge rate constant for charged MEH-PPV. With the probabilities of injection and discharge, these values are compared against a random number ($R(j)$) between 0 and 1 as follows. if $R(j) \leq 1 - P_U(j-1) - P_D(j-1)$ then there is no net change in charge, i.e., $C(j) = C(j-1)$, if $1 - P_U(j-1) - P_D(j-1) < R(j) < 1 - P_U(j-1)$, then the charge is reduced by one, i.e., $C(j) = C(j-1) - 1$, and finally, if $R(j) > 1 - P_U(j-1)$, then the charge is increased by $C(j) = C(j-1) + 1$.

Monte Carlo simulations as described above were performed where the number of charges on a molecule was calculated and the subsequent fluorescence intensity was calculated from a Stern−Volmer expression. The results of these simulations are shown in Figure 7C and D, where Figure 7C shows the accumulated sum of all the individual transients generated by the model and the panels of Figure 7D are the intensity histograms from the transients generated by the model. A comparison of the experimentally obtained transients and the ones generated by the Monte Carlo simulation demonstrate good

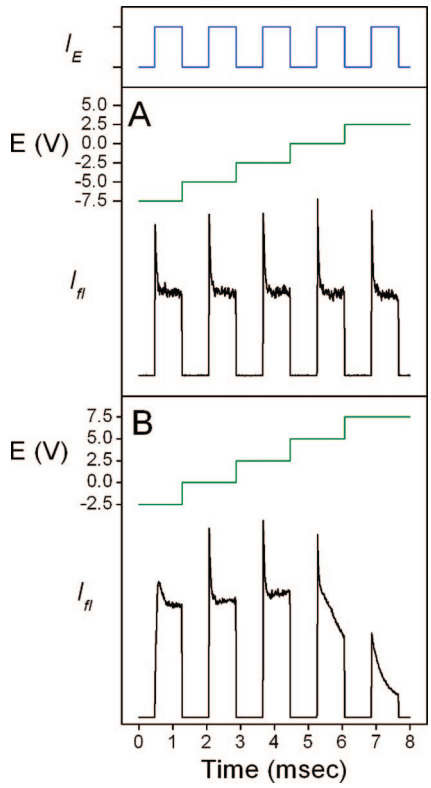


**Figure 8.** Time-averaged fluorescence-intensity transients obtained while modulating the light and bias during each cycle. The light pulse consisted of five 200 W/cm$^2$ intensity pulses of equal duration as shown by the upper blue curve. The bias was increase stepwise in 2.5 V increments as shown by the green curves. The black curves are the corresponding time-averaged fluorescence intensity transients of the same single molecule where the bias ranged from −7.5 to 2.5 V (A) and from −2.5 to 7.5 V (B) Transients are an accumulation of 1500 8-ms cycles obtained with a laser intensity of 300 W/cm$^2$.

agreement, suggesting that a small number of charges is indeed responsible for the quenching observed in the single molecules fluorescence.

***Fast Double Modulation.*** This laboratory recently introduced fast double modulation experiments similar to those presented here that are designed to monitor the lifetime and behavior of the triplet excitons of single conjugated polymer molecules that also contain holes.[58,59] Figure 8A shows the fluorescence vs time curves for a bias range for which no holes are injected in the polymer chain at any point in the sequence. In these experiments, the initial peak in fluorescence intensity at the beginning of each light pulse corresponds to a single chain with no triplets present. (The dark time period that precedes each light pulse is sufficiently long to ensure the decay of all triplet excitons.) The initial peak in the fluorescence intensity is followed by a decay for each pulse in Figure 8A due to the creation of a triplet exciton in the chain which quenchs singlet excitons and reduces the fluorescence intensity, as discussed in detail previously.

Modulation of the device bias sufficient to inject holes while taking these measurements provides information on the nature of hole-triplet interaction. Double modulation experiments were performed on our CBP devices and the results are portrayed in Figure 8. In Figure 8A, the bias threshold was increase from −7.5 to 2.5 V in a step-like fashion. The bias range is below the threshold voltage for charge injection into the CBP layer. The results are that only triplet quenching of the singlet exciton occurs, similar to when no bias is applied to the device. In contrast when a bias higher than the threshold of injection is

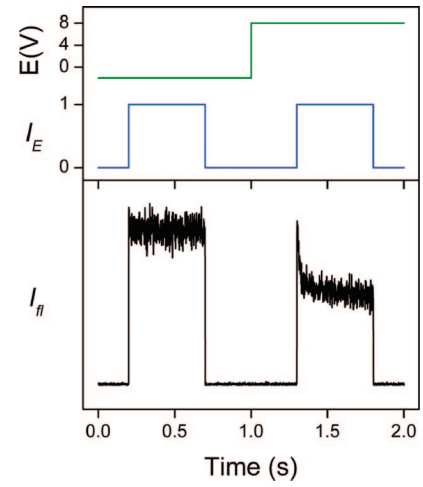


**Figure 9.** Time-averaged fluorescence-intensity transient (black curve) obtained from a single-molecule F8BT device with the applied bias (green curve) and light sequence (blue curve) as shown in the top panel. The presented transient is an accumulation of 20 2-s cycles obtained with a laser intensity of 1 W/cm$^2$.

applied as shown in Figure 8B, triplet quenching is observed to occur as well as quenching resulting from hole injection from the charged CBP layer. It is interesting to note that consistent with previous results, at higher biases, the peak corresponding to triplet quenching of the singlet exciton disappears followed by a further overall intensity decrease. This is interpreted much like previous reports in that the triplets are more efficiently quenched by holes than the singlets and thus the initial peak in fluorescence intensity disappears at higher biases. The further overall intensity drop at even higher biases is assigned to quenching of singlet excitons due to the injection of holes. These findings suggest that while holes quench triplets before singlets, the mechanism for the quenching of the singlets are most likely unrelated to the triplets. Further studies performed in a vacuum chamber microscope provide more evidence that the quenching observed in these studies is unrelated to the triplet state of the molecule. Oxygen has been observed to be a quencher of triplets, and when a pressure of 5 torr of $O_2$ was introduced into the vacuum chamber, fluorescence intensity assigned to triplets vanished.[58,60] F-V measurements showed little change in the quenching behavior due to the presence of holes, again supporting the idea that triplets are not involved in the LIHT quenching mechanism.

**3.3. SM F8BT Comparison.** To determine if the LIHT mechanism is a product of a particular combination of HTL and conjugated single molecule, CBP devices were fabricated with F8BT single molecules to provide a comparison. Bulk F8BT has a much higher HOMO energy (ionization potential) of 5.8−5.9 eV[61,62] relative to vacuum compared to MEH-PPV and thus it should be more difficult to inject the same number of holes into single-molecule F8BT. Multibias pulsed experiment results are shown in Figure 9 for a single-molecule F8BT/CBP device. From this it is shown that the charging process for single-molecule F8BT is completely light driven similar to single-molecule MEH-PPV. Similar to MEH-PPV, more intense illumination results in faster fluorescence quenching, but the quenching depth remains fixed for a given applied bias. Also of note, in similar device geometries, an applied bias of 6 V in an MEH-PPV device resulted in near complete quenching of the molecule, suggesting a single molecule has multiple charges isolated on it. At an applied bias of 8 V, the quenching of an F8BT single molecule is ∼50%, similar to the reported

quenching depth of a single hole on an F8BT molecule of similar size.[63] This finding is in agreement with the higher HOMO energy of F8BT relative to MEH-PPV. Also of interest, it appears that the LIHT mechanism is not limited to specific systems, i.e., different single molecule systems can be used as the oxidized species in these devices.

## Conclusions

Single-chain conjugated polymers were imbedded at the HTL/insulator interface of an MIS device and hole injection was observed from the HTL using an indirect fluorescence quenching technique. A series of pulsed light experiments were used to determine that light-induced hole injection dominated the charging of the single polymer chain devices with no charging occurring in the dark. This stands in contrast to the thermionic charge injection observed for bulk MEH-PPV films in similar device geometries. This difference is attributed to the possible change in the HOMO energy level and therefore, effective Schottky barrier of a single polymer chain as compared to that of a bulk film. Kinetic studies of the single-chain fluorescence quenching reveal evidence of a cooperative charging effect reminiscent to the bias stress dynamics observed in some organic transistors. This suggests that a modification of the polymer chain occurs prior to charge injection, however whether this modification is conformational or chemical in nature will require further experiments. These findings suggest that the optical preparation of trapped charge may have serious implications for the functioning of organic devices.

**Acknowledgment.** We gratefully acknowledge support by the Basic Energy Sciences Program of the Department of Energy, the National Science Foundation, Welch foundation, and the Air force Office of Scientific Research.



## References and Notes

(1) Giebeler, C.; Whitelegg, S. A.; Campbell, A. J.; Liess, M.; Martin, S. J.; Lane, P. A.; Bradley, D. D. C.; Webster, G.; Burn, P. L. *Appl. Phys. Lett.* **1999**, *74*, 3714.
(2) Feller, F.; Geschke, D.; Monkman, A. P. *J. Appl. Phys.* **2003**, *93*, 2884.
(3) Meier, M.; Karg, S.; Zuleeg, K.; Brutting, W.; Schwoerer, M. *J. Appl. Phys.* **1998**, *84*, 87.
(4) Seeley, A. J. A. B.; Friend, R. H.; Kim, J.-S.; Burroughes, J. H. *J. Appl. Phys.* **2004**, *96*, 7643.
(5) Yakimov, A. V.; Savvate'ev, V. N.; Davidov, D. *Synth. Met.* **2000**, *115*, 51.
(6) Salleo, A.; Street, R. A. *J. Appl. Phys.* **2003**, *94*, 471.
(7) Gundlach, D. J.; Jackson, T. N.; Schlom, D. G.; Nelson, S. F. *Appl. Phys. Lett.* **1999**, *74*, 3302.
(8) Salleo, A.; Street, R. A. *Phys. Rev. B* **2004**, *70*, 235324/1.
(9) Muller, E. M.; Marohn, J. A. *Adv. Mater.* **2005,** *17*,1410.
(10) Jaquith, M.; Muller, E. M.; Marohn, J. A. *J. Phys. Chem. B* **2007**, *111*, 7711.
(11) Northrup, J. E.; Chabinyc, M. L. *Phys. Rev. B* **2003**, 68.
(12) Rep, D. B. A.; Morpurgo, A. F.; Sloof, W. G.; Klapwijk, T. M. *J. Appl. Phys.* **2003**, *93*, 2082.
(13) Zilker, S. J.; Detcheverry, C.; Cantatore, E.; de Leeuw, D. M. *Appl. Phys. Lett.* **2001**, *79*, 1124.
(14) Gomes, H. L.; Stallinga, P.; Rost, H.; Holmes, A. B.; Harrison, M. G.; Friend, R. H. *Appl. Phys. Lett.* **1999**, *74*, 1144.
(15) Matters, M.; De Leeuw, D. M.; Herwig, P. T.; Brown, A. R. *Synth. Met.* **1999**, *102*, 998.
(16) Goldmann, C.; Gundlach, D. J.; Batlogg, B. *Appl. Phys. Lett.* **2006**, *88*, 063501/1.
(17) Kagan, C. R.; Afzali, A.; Graham, T. O. *Appl. Phys. Lett.* **2005**, 86.
(18) Jurchescu, O. D.; Baas, J.; Palstra, T. T. M. *Appl. Phys. Lett.* **2005**, 87.
(19) Lupton, J. M.; Nikitenko, V. R.; Samuel, I. D. W.; Bassler, H. *J. Appl. Phys.* **2001**, *89*, 311.
(20) Sinha, S.; Monkman, A. P. *J. Appl. Phys.* **2005**, 97.
(21) Chang, J. B.; Subramanian, V. *Appl. Phys. Lett.* **2006**, *88*, 233513/1.
(22) Gomes, H. L.; Stallinga, P.; Dinelli, F.; Murgia, M.; Biscarini, F.; de Leeuw, D. M.; Muck, T.; Geurts, J.; Molenkamp, L. W.; Wagner, V. *Appl. Phys. Lett.* **2004**, *84*, 3184.
(23) Lang, D. V.; Chi, X.; Siegrist, T.; Sergent, A. M.; Ramirez, A. P. *Phys. Rev. Lett.* **2004**, *93*, 076601/1.
(24) Kadashchuk, A.; Schmechel, R.; von Seggern, H.; Scherf, U.; Vakhnin, A. *J. Appl. Phys.* **2005**, *98*, 024101/1.
(25) Muller, J. G.; Lemmer, U.; Feldmann, J.; Scherf, U. *Phys. Rev. Lett.* **2002**, 88.
(26) Bolinger, J. C.; Fradkin, L.; Lee, K.-J.; Palacios, R. E.; Barbara, P. F. *Proc. Natl. Acad. Sci. U.S.A.*, submitted for publication.
(27) Burrows, P. E.; Bulovic, V.; Forrest, S. R.; Sapochak, L. S.; Mccarty, D. M.; Thompson, M. E. *Appl. Phys. Lett.* **1994**, *65*, 2922.
(28) Yip, W. T.; Hu, D. H.; Yu, J.; Vanden Bout, D. A.; Barbara, P. F. *J. Phys. Chem. A* **1998**, *102*, 7564.
(29) Gesquiere, A. J.; Park, S. J.; Barbara, P. F. *J. Phys. Chem. B* **2004**, *108*, 10301.
(30) Hill, I. G.; Kahn, A. *J. Appl. Phys.* **1999**, *86*, 4515.
(31) Wang, Y.; Gao, W. Y.; Braun, S.; Salaneck, W. R.; Amy, F.; Chan, C.; Kahn, A. *Appl. Phys. Lett.* **2005**, 87.
(32) Baldo, M. A.; Thompson, M. E.; Forrest, S. R. *Nature* **2000**, *403*, 750.
(33) Matsusue, N.; Ikame, S.; Suzuki, Y.; Naito, H. *Appl. Phys. Lett.* **2004**, *85*, 4046.
(34) Liang, C. J.; Zhao, D.; Hong, Z. R.; Zhao, D. X.; Liu, X. Y.; Li, W. L.; Peng, J. B.; Yu, J. Q.; Lee, C. S.; Lee, S. T. *Appl. Phys. Lett.* **2000**, *76*, 67.
(35) Hong, Z. R.; Liang, C. J.; Li, R. G.; Li, W. L.; Zhao, D.; Fan, D.; Wang, D. Y.; Chu, B.; Zang, F. X.; Hong, L. S.; Lee, S. T. *Adv. Mater.* **2001**, *13*, 1241.
(36) Palacios, R. E.; Fan, F. R. F.; Grey, J. K.; Suk, J.; Bard, A. J.; Barbara, P. F. *Nat. Mater.* **2007**, *6*, 680.
(37) McNeill, J. D.; Kim, D. Y.; Yu, Z.; O'Connor, D. B.; Barbara, P. F. *J. Phys. Chem. B* **2004**, *108*, 11368.
(38) Yu, J.; Song, N. W.; McNeill, J. D.; Barbara, P. F. *Isr. J. Chem.* **2004**, *44*, 127.
(39) Palacios, R. E.; Fan, F.-R. F.; Bard, A. J.; Barbara, P. F. *J. Am. Chem. Soc.* **2006**, *128*, 9028.
(40) Park, S.-J.; Gesquiere, A. J.; Yu, J.; Barbara, P. F. *J. Am. Chem. Soc.* **2004**, *126*, 4116.
(41) Lee, Y. J.; Park, S.-J.; Gesquiere, A. J.; Barbara, P. F. *Appl. Phys. Lett.* **2005**, *87*, 051906/1.
(42) Schindler, F.; Lupton, J. M.; Mueller, J.; Feldmann, J.; Scherf, U. *Nat. Mater.* **2006**, *5*, 141.
(43) Smith, T. M.; Kim, J.; Peteanu, L. A.; Wildeman, J. *J. Phys. Chem. C* **2007**, *111*, 10119.
(44) Smith, T. M.; Hazelton, N.; Peteanu, L. A.; Wildeman, J. *J. Phys. Chem. B* **2006**, *110*, 7732.
(45) Hania, P. R.; Thomsson, D.; Scheblykin, I. G. *J. Phys. Chem. B* **2006**, *110*, 25895.
(46) Hania, P. R.; Scheblykin, I. G. *Chem. Phys. Lett.* **2005**, *414*, 127.
(47) Devine, R. A. B.; Ling, M.-M.; Mallik, A. B.; Roberts, M.; Bao, Z. *Appl. Phys. Lett.* **2006**, *88*, 151907/1.
(48) Berleb, S.; Brutting, W.; Paasch, G. *Org. Electron.* **2000**, *1*, 41.
(49) Berleb, S.; Brutting, W.; Paasch, G. *Synth. Met.* **2001**, *122*, 37.
(50) Lindner, T.; Paasch, G.; Scheinert, S. *J. Appl. Phys.* **2005**, *98*, 114505/1.
(51) Hieda, H.; Tanaka, K.; Naito, K.; Gemma, N. *Thin Solid Films* **1998**, *331*, 152.
(52) Kim, Y. G.; Thompson, B. C.; Ananthakrishnan, N.; Padmanaban, G.; Ramakrishnan, S.; Reynolds, J. R. *J. Mater. Res.* **2005**, *20*, 3188.
(53) Friedlein, R.; Crispin, X.; Salaneck, W. R. *J. Power Sources* **2004**, *129*, 29.
(54) Amy, F.; Chan, C.; Kahn, A. *Org. Electron.* **2005**, *6*, 85.
(55) Gruhn, N. E.; da Silva, D. A.; Bill, T. G.; Malagoli, M.; Coropceanu, V.; Kahn, A.; Bredas, J. L. *J. Am. Chem. Soc.* **2002**, *124*, 7918.
(56) Sato, N.; Inokuchi, H.; Silinsh, E. A. *Chem. Phys.* **1987**, *115*, 269.
(57) Devine, R. A. B. *J. Appl. Phys.* **2006**, *99*, 083701/1.
(58) Gesquiere, A. J.; Park, S.-J.; Barbara, P. F. *J. Am. Chem. Soc.* **2005**, *127*, 9556.
(59) Palacios, R. E.; Barbara, P. F. *J. Fluoresc.* **2007**, *17*, 749.
(60) Fradkin, L.; Bolinger, J. C.; Lee, K. J.; Palacios, R. E.; Barbara, P. F. Manuscript in preparation.
(61) Fung, M. K.; Lai, S. L.; Tong, S. W.; Bao, S. N.; Lee, C. S.; Wu, W. W.; Inbasekaran, M.; O'Brien, J. J.; Lee, S. T. *J. Appl. Phys.* **2003**, *94*, 5763.
(62) Chua, L. L.; Zaumseil, J.; Chang, J. F.; Ou, E. C. W.; Ho, P. K. H.; Sirringhaus, H.; Friend, R. H. *Nature* **2005**, *434*, 194.
(63) Lammi, R. K.; Barbara, P. F. *Photochem. Photobiol. Sci.* **2005**, *4*, 95.

JP804901S